

Kondo effect in f -electron superlattices

Robert Peters,^{1,*} Yasuhiro Tada,² and Norio Kawakami¹

¹*Department of Physics, Kyoto University, Kyoto 606-8502, Japan*

²*Institute for Solid State Physics, The University of Tokyo, Kashiwa 277-8581, Japan*

(Dated: July 3, 2018)

We demonstrate the importance of the Kondo effect in artificially created f -electron superlattices. We show that the Kondo effect does not only change the density of states of the f -electron layers, but is also the cause of pronounced resonances at the Fermi energy in the density of states of the non-interacting layers in the superlattice, which are between the f -electron layers. Remarkably, these resonances strongly depend on the structure of the superlattice; due to interference, the density of states at the Fermi energy can be strongly enhanced or even shows no changes at all. Furthermore, we show that by inserting the Kondo lattice layer into a three-dimensional (3D) metal, the gap of the Kondo insulating state changes from a full gap to a pseudo gap with quadratically vanishing spectral weight around the Fermi energy. Due to the formation of the Kondo insulating state in the f -electron layer, the superlattice becomes strongly anisotropic below the Kondo temperature. We prove this by calculating the in-plane and the out-of-plane conductivity of the superlattice.

PACS numbers: 71.10.Fd; 71.27.+a; 73.21.Cd; 75.20.Hr; 75.30.Mb

I. INTRODUCTION

Recently, remarkable progress has been made in the creation of artificial superlattices including f -electron materials.¹⁻³ These superlattices consist of a periodic arrangement of two-dimensional f -electron layers, which are inserted into a different material. In the experiments, these superlattices show some intriguing magnetic and superconducting properties, which are tunable by changing the superlattice structure. For example, the Néel temperature in CeIn₃(n)/LaIn₃(4) superlattices¹ decreases to zero when the Cerium layer thickness n is reduced to $n = 2$, which is accompanied by a linear temperature dependence of the resistivity. In other experiments, using the heavy fermion CeCoIn₅ and the conventional metal YbCoIn₅, a two-dimensional strong coupling superconducting state has been observed.² Also in these experiments, the transition temperature and the magnetic field dependence are strongly affected by the structure of the superlattice. The ability to create new materials with properties that depend on the superlattice structure may provide the possibility to construct new functional devices.

In f -electron materials, the competition or cooperation of two mechanisms mainly determines the properties of the material, i.e. the Kondo effect and the RKKY interaction.⁴ The quantum criticality arising when both effects are equally strong, causes non-Fermi liquid behavior and unconventional superconductivity.⁵⁻⁷ In order to understand these intriguing effects in the context of these superlattices, it is essential to understand how both mechanisms, which are the cause of most of the phenomena, are influenced by the superlattice structure. Therefore, in this paper we will study the Kondo effect in the paramagnetic state of f -electron superlattices. We will clarify how the Kondo effect influences the f -electron layers and in what way the Kondo effect is observable in the non-interacting layers, which are in between the

f -electron layers. Another interesting question which we will address is the influence of the superlattice structure on the low energy behavior of a Kondo lattice: What happens to the full gap of the isolated Kondo lattice layer, when it is coupled to metallic layers.

In order to answer these questions, an essential point is the proper treatment of the superlattice structure. Therefore, we simulate systems which include two-dimensional (2D) f -electron layers and 2D non-interacting layers. The number and order of these layers can be varied, so that a variety of different superlattices can be studied. We are thus able to analyze these f -electron superlattices and the Kondo effect within these systems taking the structure of the superlattice fully into account. We find that the hybridization gap in the f -electron layers changes into a pseudo gap as soon as different layers are coupled to each other. However, the Kondo effect in the f -electron layers also strongly affects the density of states of the non-interacting layers, corresponding to Yb- or La-layers in the above-mentioned experiments. We find that resonances, whose shapes depend on the superlattice structure and are influenced by interference from different f -electron layers, appear at the Fermi energy. These resonances have strong influence on the local properties of these superlattices and might be observable by local probes in experiments.

The remainder of this paper is organized as follows: In the next section, we explain in detail the model and the method which we use in our study. This is followed by a section where we study a single f -electron layer within a 3D lattice. This kind of study will give insights into the physics which can be expected in the superlattice. Finally, we present results for the paramagnetic state in f -electron superlattices, analyzing a wide range of different superlattice structures. A summary will conclude this paper.

II. MODEL AND METHOD

We simulate a three dimensional system, consisting of a periodic arrangement of f -electron- and non-interacting layers, see Fig. 1. The Hamiltonian of the superlattice can be written as a sum of terms describing 2D non-interacting layers, H_{NIL} , f -electron layers described by a 2D Kondo lattice model,^{4,8,9} H_{KLL} , and a hopping, H_{Inter} , which connects adjacent layers with each other:

$$\begin{aligned} H &= H_{\text{NIL}} + H_{\text{KLL}} + H_{\text{Inter}}, \\ H_{\text{NIL}} &= t_{\text{NIL}} \sum_{\langle i,j \rangle \sigma} c_{iz\sigma}^\dagger c_{jz\sigma}, \\ H_{\text{KLL}} &= t_{\text{KLL}} \sum_{\langle i,j \rangle \sigma} c_{iz\sigma}^\dagger c_{jz\sigma} + J \sum_i \vec{S}_{iz} \cdot \vec{s}_{iz}, \\ H_{\text{Inter}} &= t_z \sum_i \sum_{\langle z_1, z_2 \rangle \sigma} c_{iz_1, \sigma}^\dagger c_{iz_2 \sigma}. \end{aligned} \quad (1)$$

In this paper we describe each layer as a 2D square lattice for which i and j are indices within the same layer. The layer index is given by z . Thus, the operator $c_{iz\sigma}^\dagger$ creates an electron at lattice site i in layer z in spin direction σ . Besides a nearest neighbor hopping within the 3D superlattice, there is an additional spin-spin interaction, $J \sum_i \vec{S}_{iz} \cdot \vec{s}_{iz}$, between the spin of the electrons and the localized spins in the Kondo lattice layers. If not otherwise stated, all hopping constants are equal $t_{\text{NIL}} = t_{\text{KLL}} = t_z = t$. We take the 2D half-bandwidth $W_2 = 4t$ as unit of energy. Furthermore, we assume throughout this paper an antiferromagnetic coupling, $J > 0$, between the conduction electrons and the localized spins, which is appropriate to describe heavy fermion materials. Without any coupling to the spins in the Kondo lattice model, the system corresponds to non-interacting electrons in a 3D cubic lattice. In the rest of the paper, we will characterize the superlattice structure as (N, M) , corresponding to $\text{KLL}_N/\text{NIL}_M$ (N : Kondo lattice layers (KLL), M : non-interacting layers (NIL)). While we assume that the system is homogeneous within each plane, i.e. within the same plane all lattice sites are equal, we use open boundary conditions perpendicular to the layered structure including up to 40 layers in the superlattice. Throughout the paper, we focus on physical properties of the center-layers, which do not show any signs of boundary effects.

For solving this model, we use a combination of the inhomogeneous dynamical mean field theory (IDMFT) and the numerical renormalization group (NRG).^{10,11} IDMFT originates in the dynamical mean field theory (DMFT).¹² While non-local contributions to the self-energy are neglected, local fluctuations and the layer dependence of the self-energy are fully taken into account within IDMFT. The Kondo effect as well as the heavy fermion state are well described, and the phase diagram of the Kondo lattice model within DMFT has been investigated by a number of authors before.¹³⁻²³

In the original DMFT approach, one is interested in a

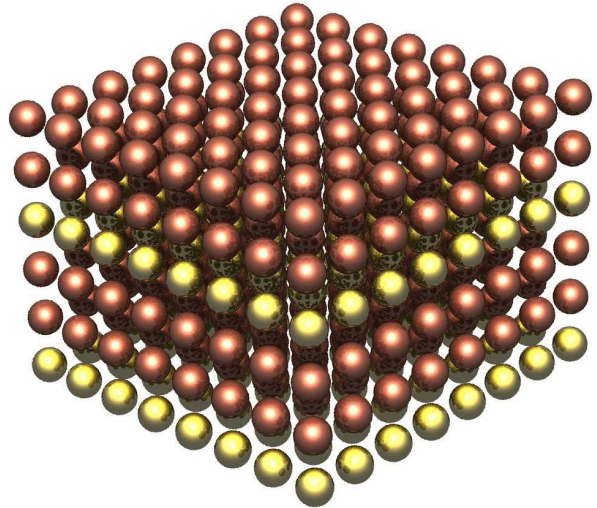


Figure 1: (Color online) Schematic picture of a (1,2)-superlattice, consisting of a periodic arrangement of one f -electron layer and two non-interacting layers.

homogeneous lattice, so that each site can be described by the same self-energy. Because in the superlattice the system is inhomogeneous, i.e. there are different kinds of layers with different physical properties, different lattice sites cannot be approximated with the same self-energy. Instead, we have to take into account the structure of the superlattice and calculate a site dependent self-energy. In the case of the f -electron superlattice, Eq. (1), the self-energy for the NILs vanishes. IDMFT works as follows:

a) We start with a guessed self-energy, which can also be set to zero.

b) Using this self-energy, we calculate the site dependent local Green's functions of the superlattice. Because our system is translation invariant within each layer, we use Fourier transformation for lattice sites within the same layer. The local Green's function of layer z , $G_z(\omega + i\eta)$, thus reads

$$G_z(\omega + i\eta) = \frac{1}{4\pi^2} \int dk_x dk_y \left((\omega + i\eta) \mathbb{I} - H(k_x, k_y) - \Sigma(\omega + i\eta)_z \right)^{-1}, \quad (2)$$

where $H(k_x, k_y)$ is a matrix corresponding to the one-particle Hamiltonian of the system, i.e. Eq. (1) with $J = 0$, in which for the in-plane hopping Fourier transformation has been used, resulting in $H_{\text{NIL}} = 2t(\cos(k_x) + \cos(k_y))$. Eq. (2) involves a matrix inversion of dimension corresponding to the number of layers in the system. Interaction effects are taken into account by the self-energy $\Sigma(\omega + i\eta)$, which depends on the layer. Furthermore, we take η small enough, so that the resulting Kondo gap can be described. A typical value in our calculations is $\eta = 10^{-5}$.

c) We now relate the calculated local Green's function

of each layer with the Green's function of the corresponding quantum impurity model using the same self-energy. The impurity Green's function can be written as²⁴

$$G_{\text{IMP}}(\omega + i\eta) = \frac{1}{\omega + i\eta - \Delta(\omega + i\eta) - \Sigma(\omega + i\eta)}. \quad (3)$$

$\Delta(\omega + i\eta)$ is the hybridization between the impurity site and the conduction electron bath. Due to the locality of the self-energy, we can assume that the calculated lattice Green's function is equal to the impurity Green's function, from which we can determine the hybridization function

$$\Delta(\omega + i\eta) = \omega + i\eta - G_z^{-1}(\omega + i\eta) - \Sigma(\omega + i\eta). \quad (4)$$

Within IDMFT, the hybridization function, $\Delta(\omega + i\eta)$, depends on the layer.

d) The calculated hybridization functions define for each layer a quantum impurity model. We solve for each layer the corresponding impurity model and calculate its self-energy.

e) We iterate this procedure by calculating new local lattice Green's functions, see *b)*. If the self-energies of all layers between two iterations do not change, the IDMFT solution is found.

Besides the calculation of local Green's functions, the time consuming step is the calculation of the self-energy for each layer. For this purpose we use the NRG.¹¹ The NRG is able to solve these quantum impurity models for a wide range of temperatures and is able to resolve exponentially small energy scales like the Kondo resonance using the complete Fock space algorithm.^{25,26} Throughout this paper, we use a discretization parameter $\Lambda = 2$ and keep $N = 1000$ states within each NRG iteration.¹¹

III. A SINGLE 2D KONDO LATTICE LAYER WITHIN A 3D METALLIC HOST

In this section, we will first analyze a single KLL within a 3D metal. This will give insights into changes occurring due to the insertion of a KLL into a metallic host.

The paramagnetic Kondo lattice model at half filling exhibits a gap in the density of states (DOS) at the Fermi energy. The system is in the Kondo insulating state. The first question, we want to clarify is, how the DOS of the Kondo lattice is modified, if it is inserted into a 3D metal. What happens to the full gap, if it is coupled to a metallic layer? The electrons of the metallic layer may tunnel into the KLL, thus, modifying the DOS.

We show the DOS of a single KLL within a 3D metal for different inter-layer hopping amplitudes, t_z , in the upper panel of Fig. 2. The insets show magnifications around the Fermi energy. First, when increasing the inter-layer hopping amplitude, the gap width decreases. Second, the double-logarithmic inset clearly shows that the spectral weight vanishes as a power law for small frequencies, if the KLL is coupled to a metallic layer. The

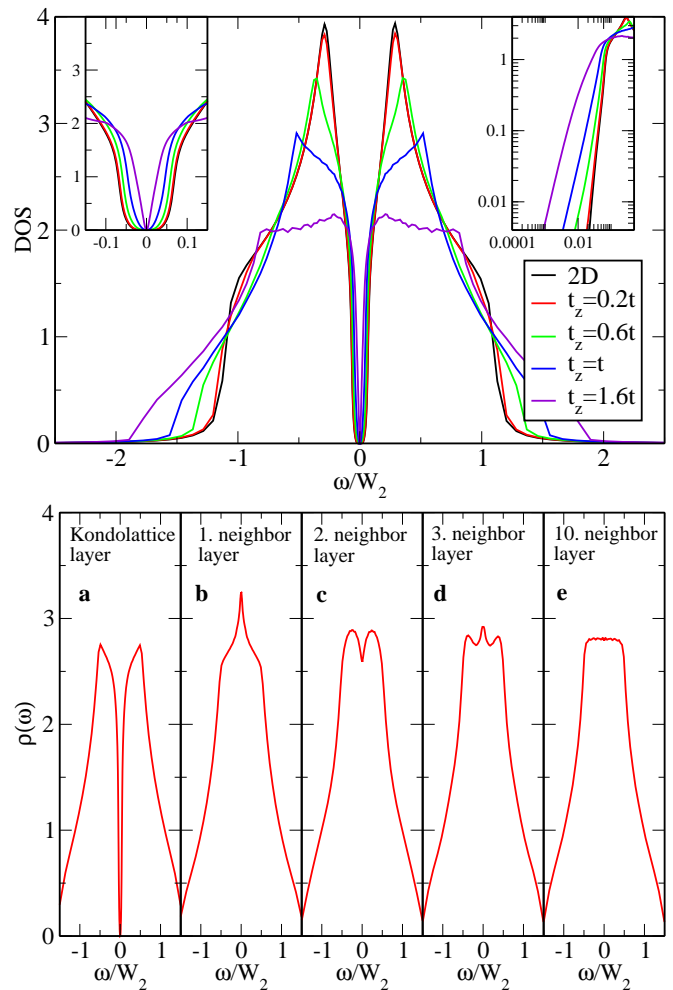


Figure 2: (Color online) Results of a single KLL, $J = 0.5W_2$, within a 3D non-interacting host. Upper panel: DOS of the KLL for different hopping amplitudes, t_z , between the KLL and the NIL. The insets show magnifications around the Fermi energy. Lower panel: DOS of different layers. a) DOS of the KLL, b) nearest neighbor layer, c) next nearest neighbor layer, d) third-nearest neighbor layer, e) 10 layers away.

determined exponent is approximately two and seems to be independent of the hopping amplitude. The prefactor in front of the quadratic term, however, does depend on the hopping amplitude and increases with increasing hopping. An arbitrary small coupling, $|t_z| > 0$, between different layers is sufficient to transform the full gap of an isolated KLL into a pseudo gap. We note here that even for the isolated KLL the edges of the gap are broadened due to interaction effects.

Another noticeable change occurs in the DOS away from the Fermi energy. Increasing the coupling between the KLL and the NILs, the two-peak structure, which is a remnant of the van Hove singularity in the two-dimensional square lattice, is flattened and vanishes. The hopping between different layers creates a 3D structure for the conduction electrons, and thus destroys these sin-

gularities.

To get some more insights into the formation of the pseudo gap, we look at a non-interacting analog, consisting of two layers, which are coupled via hopping t . While one layer is a non-interacting metallic layer, the other layer is described by a non-interacting periodic Anderson model. In the periodic Anderson model each lattice site is hybridized via a hopping V to a localized f -electron level. The model can be written as

$$H = \sum_{ij,\sigma} t_{ij} c_{i\sigma}^\dagger c_{j\sigma} + V \left(c_{i\sigma}^\dagger f_{i\sigma} + f_{i\sigma}^\dagger c_{i\sigma} \right),$$

where $f_{i\sigma}^\dagger$ creates an f -electron. Due to this hybridization, a gap opens around the Fermi energy. In the case of the non-interacting periodic Anderson model, the spectral weight at the edges of the gap jumps from a finite value to zero. For the Kondo lattice model, this jump is smeared out due to two-particle interactions between the conduction electrons and the localized spins. If the layer described by the periodic Anderson model is coupled to the metallic layer via a hopping t , the DOS can be written as

$$\rho(\omega) = \int_{-D}^D d\epsilon \frac{1}{\omega + i0 - \epsilon - \frac{V^2}{\omega + i0} - \frac{t^2}{\omega + i0 - \epsilon}},$$

where we have assumed for simplicity a constant DOS within each layer. The result of this integral shows that the gap of the f -electron layer is changed by the coupling to a metallic layer from a full gap to a pseudo gap. The existence of the gap itself is unchanged. The local hybridization within the f -electron layer is sufficient to open a gap. However, inside the original gap, we find that the spectral weight vanishes quadratically. The change between a full gap and the pseudo gap occurs at arbitrary small hopping between these two layers and happens in the same way in the interacting Kondo lattice model and the non-interacting periodic Anderson model. The exponent of the power law, which determines how the spectral weight vanishes around the Fermi energy, seems to be equal in both models.

The coupling between the KLL and the NILs does not only modify the DOS of the KLL. It has also profound influence on the DOS of the neighboring NILs. In the lower panel of Fig. 2, we show the DOS of different layers in a system, where only one KLL is inserted into a 3D metal. The hopping is isotropic, $t_z = t$. The DOS of the KLL (panel a) shows the above-described pseudo gap around the Fermi energy, $\omega = 0$. The DOS of the neighboring layer (panel b), which is a non-interacting layer, shows a modification from the usual 3D DOS; there is a peak at the Fermi energy, whose width corresponds to the gap width of the KLL. The next nearest layer, on the other hand, shows a dip at the Fermi energy. The peak or gap at the Fermi energy alternates with increasing distance from the KLL, showing typical $2k_F$ oscillations. The width of these structures at the Fermi energy is completely determined by the gap width of the KLL,

thus, they are supposed to be related to the Kondo effect (Further evidence that the Kondo effect plays a significant role is shown later). However, the amplitude of these structures decreases quickly, roughly as $1/d^\kappa$ ($\kappa \approx 1.1$, d : distance between the layers), when going further away from the KLL. These oscillations occur in a similar way as Friedel oscillations around impurities in metals. Panel e) in Fig. 2 shows the DOS of an atom 10 layers away from the KLL, where the DOS resembles the unperturbed 3D DOS.

IV. f -ELECTRON SUPERLATTICES

Next, we will study the Kondo effect in f -electron superlattices, i.e. in a periodic arrangement of 2D KLLs and NILs. Figs. 3 and 4 show results for a (1,1)-superlattice, where the system is composed alternatively of KLLs and NILs. The behavior of the DOS in this superlattice is similar to the alternating peak/dip structure at the Fermi energy of the system with a single KLL in 3D (Fig. 2). The KLL shows again the formation of a pseudo gap, and the DOS of the nearest neighbor NIL shows a peak at the Fermi energy. However, if we compare the amplitude of the peak at the Fermi energy of the NIL to the DOS of the unperturbed 3D metal, the DOS is enhanced nearly by a factor of two. Because each NIL is sandwiched by two KLLs in this (1,1)-superlattice structure, the Kondo effect of both KLLs enhances the DOS at the Fermi energy of the NIL. One may refer to this as ‘‘constructive interference’’. In Fig. 3, we also include curves for different temperatures, showing how the gap in the KLL and the peak in the NIL are built up with decreasing temperature. At high temperatures, $T \gg T_K$, where T_K is the Kondo temperature of the system, one can clearly see a dip formation in the DOS of the KLL and a bump in the DOS of the NIL. These structures are formed at temperatures $T \approx J$. When lowering the temperature below the Kondo temperature, the dip becomes more pronounced and eventually forms the Kondo gap, while the peak in the DOS of the NIL increases at the same time. A closer analysis of the influence of the temperature on the DOS at the Fermi energy for the (1,1)-superlattice is presented in Fig. 4. The left panel shows the DOS at the Fermi energy of both layers for different temperatures and different coupling strengths. For all coupling strengths, there is a crossover from the high temperature phase, where both layers have nearly equal weight at the Fermi energy, to the low temperature phase consisting of Kondo gapped layers and NILs, which have enhanced weight at the Fermi energy. The crossover temperature, which is approximately equal to the width of the gap of the KLL or the width of the peak of the NIL at the Fermi energy, decreases with decreasing coupling strength. We show these crossover temperatures over the inverse coupling strength in the right panel of Fig. 4, proving the exponential dependence on the coupling strength J . Because the peak in the DOS of the NIL

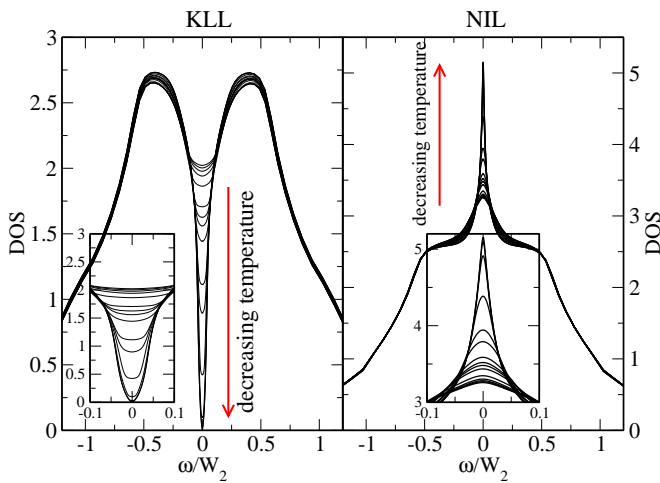


Figure 3: (Color online) DOS of a (1,1)-superlattice for different temperatures. The insets show magnifications around the Fermi energy.

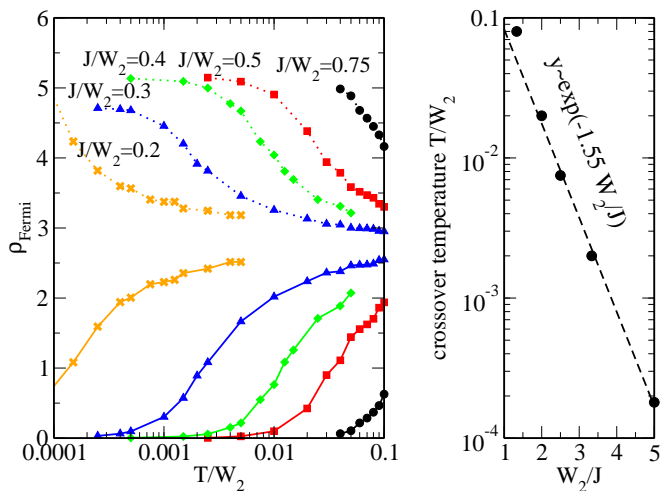


Figure 4: (Color online) DOS at the Fermi energy and crossover temperature for the (1,1)-superlattice. Left: DOS at the Fermi energy, ρ_{Fermi} for different temperatures and interaction strengths. The lower (upper) lines correspond to the KLL (NIL). Right: crossover temperature over inverse interaction strength, proving the exponential dependence.

shows the same temperature dependence as the gap of the KLL, we can state that both resonances are induced by the Kondo effect of the f -electrons. The qualitative behavior of the system is independent of the coupling strength J . The coupling strength only determines the Kondo temperature below which the resonances at the Fermi energy can be observed, as long as a paramagnetic state is formed.

If the structure of the superlattice is changed, the resonances at the Fermi energy are also altered. In Figs. 5 and 6, we show the temperature dependent DOS of the (1,2)- and (1,3)-superlattices, which consist of two or three NILs in the unit cell, respectively. For both

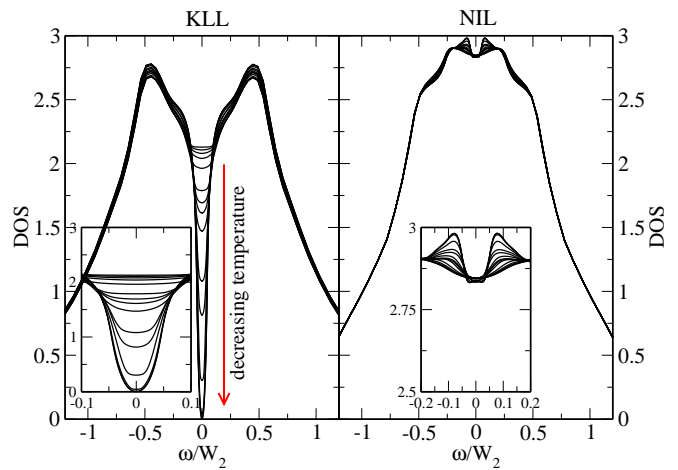


Figure 5: (Color online) DOS of a (1,2)-superlattice for different temperatures. Due to symmetry, both NILs are identical.

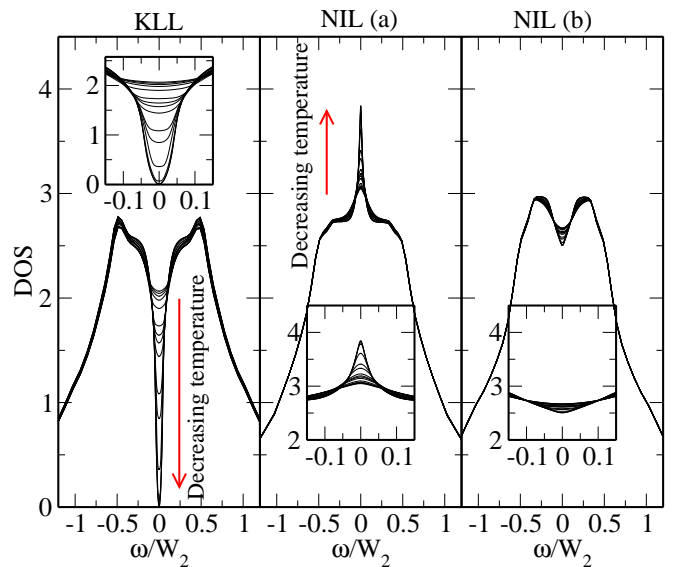


Figure 6: (Color online) DOS of a (1,3)-superlattice for different temperatures.

configurations, the KLLs form the pseudo gap at the Fermi energy at low temperatures. This behavior is not changed by tuning the structure of the superlattice. Independent of the superlattice structure, the KLLs always form Kondo gapped states at half filling and zero temperature. The NILs, on the other hand, show different behavior depending on the superlattice structure. For the (1,2)-superlattice in Fig. 5, both non-interacting layers exhibit identical DOS, because of the symmetry of the system. Surprisingly, the DOS at the Fermi energy of the NILs remains unchanged for all temperatures. This is in contrast to the (1,1)-superlattice configuration shown in Fig. 3. In the (1,2)-superlattice, we observe only small temperature-dependent changes away from the Fermi energy, $\omega \approx \pm 0.1W_2$ in Fig. 5, but there is no peak or dip at

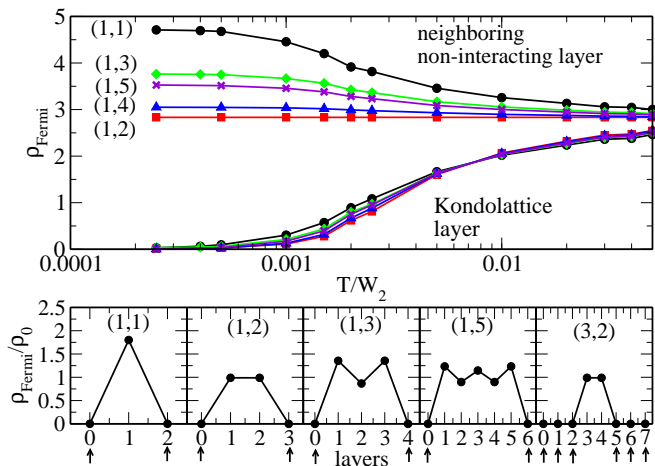


Figure 7: (Color online) Upper panel: DOS at the Fermi energy over temperature for $J/W_2 = 0.3$, and for variety of superlattice configurations. We only show the Kondo lattice layer and the nearest neighboring NIL. Lower panel: Each panel shows the normalized DOS at the Fermi energy for all different layers in the superlattice. The arrows at the layer index denote the KLLs.

the Fermi energy. This can be explained by the peak/dip oscillations seen in the DOS of a single KLL in 3D, shown in Fig. 2. The nearest neighbor NIL exhibits a peak at the Fermi energy, while the next nearest layer shows a dip. In the (1,2)-superlattice, there is thus a “destructive interference” of both effects. Each NIL is nearest neighbor as well as next nearest neighbor to a KLL. This results in an unaltered DOS of the NIL at the Fermi energy. Therefore, the influence of the Kondo effect on the DOS at the Fermi energy is only visible in the KLLs for this configuration. The situation is again changed for a (1,3)-superlattice, shown in Fig. 6. This structure favors a constructive interference. Thus, while the KLL forms the Kondo gap, the NIL which is nearest to the KLL shows a peak at the Fermi energy. The peak height is reduced compared to the (1,1)-superlattice (see Fig. 3). The second NIL, which is in the middle of three NILs, shows a small dip at the Fermi energy. This agrees with the peak/dip oscillations found in the results of a single KLL in 3D.

Finally, we compare the DOS at the Fermi energy for a variety of superlattice configurations in Fig. 7. The upper panel in Fig. 7 shows the temperature dependence of the DOS at the Fermi energy for the KLL and the nearest neighboring NIL for fixed interaction strength, $J/W_2 = 0.3$. On the one hand, any KLL forms for any superlattice configuration the Kondo gap at the Fermi energy. On the other hand, we observe that the amplitude of the peak in the neighboring NIL strongly depends on the superlattice structure, due to interference between the Kondo effect of different f -electron layers. Because of the above-described constructive/destructive interference, the peak height changes non-monotonically when inserting additional NILs, and shows even-odd oscillations. Looking

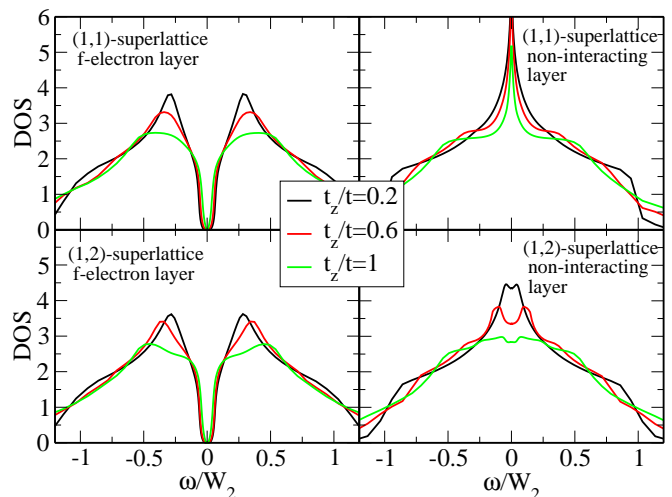


Figure 8: (Color online) Spectral functions at $T = 0$ for the (1,1)- and (1,2)-superlattice for different inter-layer couplings, t_z .

only at an odd number of NILs, which always results in a constructive interference for the nearest neighbor NIL, the peak height is decreased when inserting new NILs. The maximum peak height can be observed for the (1,1)-superlattice. On the other hand, for an even number of NILs, the peak height is increased when inserting new layers. For the (1,2)-superlattice, there is complete destructive interference and consequently no peak emerges at the Fermi energy. Furthermore, the crossover temperature seems to be slightly dependent on the superlattice structure. This is best visible in the temperature dependence of the KLLs in Fig. 7. Note that the crossover temperatures of different superlattices are changed according to the peak heights in the DOS of the NIL at the Fermi energy. The lowest crossover temperature can be observed for the (1,1)-superlattice, and the highest crossover temperature can be observed for the (1,2)-superlattice. The difference between the (1,1)- and the (1,2)-superlattice is about 20%, which should be detectable in experiments.

Up to now, we have focused on periodic configurations of a single KLL and a certain number of NILs. Thus, there are never two KLLs touching each other. The reason for our choice is that the physics, which has been so far explained, does not change when adding additional KLLs. There are only small changes in the DOS away from the Fermi energy. Any KLL forms a pseudo gap within the superlattice structure, for which the spectral weight around the Fermi energy vanishes quadratically. Only the prefactor in front of the quadratic term does depend on the superlattice structure. Furthermore, the resonances observed at the Fermi energy of the NILs, are only determined by the number of the NILs.

In the lower panel of Fig. 7, we show the changes of the DOS at the Fermi energy for all layers in different superlattices at zero temperature. As in the results

for the single KLL embedded in 3D, we observe oscillations of peaks and dips at the Fermi energy of the NILs. Configurations having two NILs are special, as described above. We observe that for these superlattices ((1,2)- and (3,2)-superlattice in Fig. 7), the DOS at the Fermi energy is not changed and is independent of the number of KLLs. For the other superlattice configurations, we see that the amplitude of the resonances decreases with inserting new NILs. However, even for the (1,5)-superlattice, where there are five NILs between the KLLs, the enhancement at the Fermi energy is still around 20%, for the (1,3)-superlattice even 40%. This shows that the Kondo effect in the f -electron layers has substantial influence on all NILs and should not be dismissed, even if there are several layers between the f -electron layers. In the experiments,¹⁻³ there are 4 or 5 NILs in between the f -electron layers. Our results imply that the Kondo effect penetrates through the NILs at low temperatures, which will lead to a coupling of the separated f -electron layers.

An open question, which we want to answer is, how the superlattice changes into a 2D system, when the inter-layer hopping is decreased. We show this process exemplary for the (1,1)- and (1,2)-superlattices in Fig. 8. With decreasing the inter-layer hopping, t_z , each layer behaves more and more like a 2D square lattice without qualitatively altering the behavior at the Fermi energy as described above. The DOS of the f -electron layer exhibits a hybridization gap at the Fermi energy. The gap width becomes slightly increased when decoupling the layers, because the gap width in the 2D Kondo lattice is larger than in the 3D Kondo lattice. The DOS of the NILs, on the other hand, is expected to evolve into the DOS of a 2D square lattice with van Hove singularity at the Fermi energy. This can be seen in the right panels of Fig. 8. For the (1,1)-superlattice, there is a peak in the DOS of the NIL for all calculated values of the inter-layer hopping. However, while in the DOS of a nearly decoupled NIL the peak corresponds to the van Hove singularity, the peak in the coupled system, $t_z/t = 1$, originates in the Kondo effect, which strongly depends on the temperature, as has been shown in Fig. 3. The spectral weight around the Fermi energy also increases for the (1,2)-superlattice. The two peak structure close to the Fermi energy remains observable but begins to merge into the van Hove singularity when decreasing the inter-layer hopping.

The formation of a gap at the Fermi energy in the DOS of the KLLs and a peak in the DOS of the NILs, results in a highly anisotropic system at low temperatures. In order to elucidate this point further, we show the real part of the frequency dependent conductivity of the (1,1)-superlattice for $J/W_2 = 0.5$ at zero temperature in Fig. 9. Writing the one-particle part of the Hamiltonian, Eq. (1), in momentum space, the current operator is given as²⁷

$$\vec{j} = e \sum_{\sigma} \sum_{\vec{k}} c_{\vec{k}\sigma}^{\dagger} \vec{v}(\vec{k}) c_{\vec{k}\sigma}, \quad (5)$$

where $\vec{v}(\vec{k}) = \frac{\partial H(k_x, k_y, k_z)}{\partial \vec{k}}$, and e is the elementary

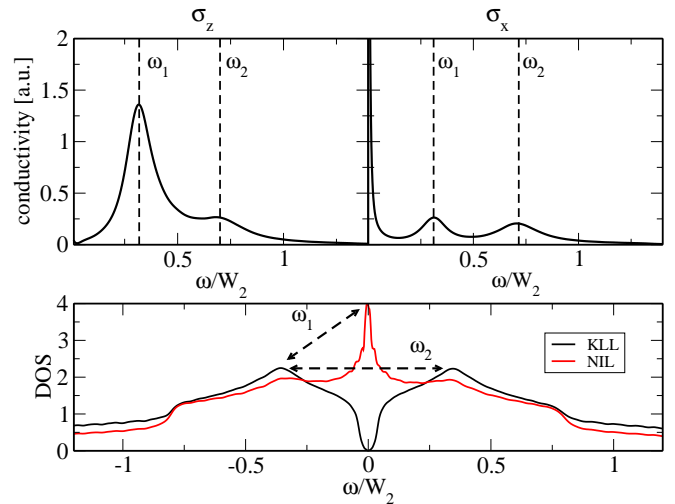


Figure 9: (Color online) Real part of the conductivity within the layers, σ_x , and perpendicular to the superlattice structure, σ_z , for $J/W_2 = 0.5$. The lower panel shows the excitations in the local DOS corresponding to the peaks in the conductivity.

charge. For calculating the conductivity, we use periodic boundary conditions in all directions. The conductivity is then given by the Kubo formula via the dynamical current-current correlation function, where the current is taken in direction μ , and reads,

$$\sigma_{\mu}(\omega) = \frac{1}{i\omega} \langle \langle j_{\mu}, j_{\mu} \rangle \rangle_{\omega+i\delta}. \quad (6)$$

Due to the locality of the self-energy within DMFT, the resulting two-particle Green's functions can be written as products of one-particle Green's functions.²⁷

In Fig. 9, we show the out-of-plane conductivity in the upper-left panel and the in-plane conductivity in the upper-right panel. The lower panel shows the local DOS of both layers. The anisotropy of the system is clearly visible in the conductivities at low frequencies. The in-plane conductivity, σ_x , exhibits a strong peak for $\omega/W_2 < 0.05$. This peak signals metallic behavior parallel to the planes. Analyzing the different components in the conductivity, we observe that this peak comes mainly from the NILs, having strong weight in the local DOS at the Fermi energy. On the other hand, the out-of-plane conductivity, σ_z , shows a gap at low frequencies. Thus, perpendicular to the layered structure the f -electron superlattice is insulating. At the Kondo temperature, the superlattice becomes strongly anisotropic, showing metallic behavior within the planes and insulating behavior perpendicular to the planes. Analyzing the conductivity at higher frequencies, we observe two distinct peaks. These two frequencies can be easily identified within the DOS of both layers (lower panel of Fig. 9); one corresponding to the excitation energies between the lower band and the central peak, and the other corresponding to the excitations between the lower and upper bands. Even if the superlattice structure is altered, the conductivity

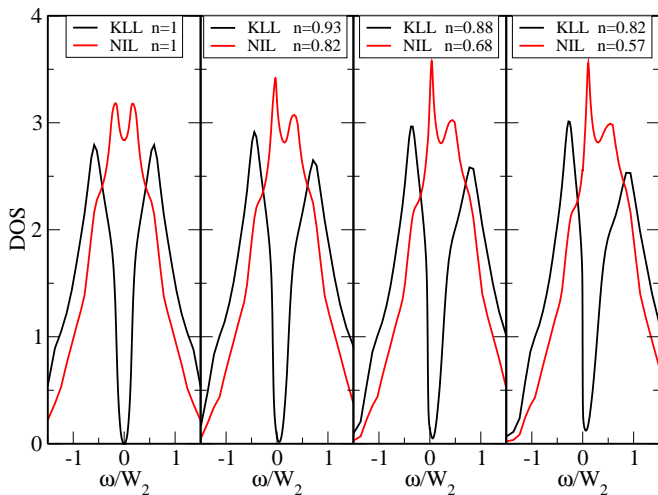


Figure 10: (Color online) DOS for the (1,2) superlattice in a doped system $J/W_2 = 0.65$.

remains qualitatively unchanged. The superlattice still behaves as an anisotropic metal at low temperatures, i.e. perpendicular to the planes the superlattice is insulating and parallel to the planes metallic. The number and position of these peaks, however, depend on the superlattice structure. At large frequencies, additional peaks are visible for different superlattice structures, arising from excitations between different layers. The temperature-dependent conductivity, especially the influence of the superlattice on it, is analyzed in detail in reference.²⁸

All results, which have been shown until now, have been for half filled lattices, for which each lattice site is occupied in average with one electron and the KLLs form the Kondo gap at the Fermi energy. If the chemical potential is changed, the system is doped away from half filling. However, the main statements about the Kondo effect, which we have made, remain valid. In Fig. 10, we show the local DOS of a (1,2)-superlattice for different chemical potentials. The structures (peaks and dips) in the DOS of the NILs are shifted. By doping the system, one of the side peaks in the DOS of the NIL is shifted towards the Fermi energy. At the same time the gap in the KLLs is shifted away from the Fermi energy. Thus, even for the doped system the Kondo effect of the f -electron superlattices is of great importance and all our previous statements about interference of the Kondo effect of different KLLs remain valid.

Furthermore, we observe that the local occupation of conduction electrons depends on the layer, see Fig. 10. Thus the system forms a charge density wave corresponding to the superlattice structure. This corresponds to the fact that different materials or different microscopic models react differently to a change of the chemical potential. Due to the local singlet formation between conduction electrons and localized spins in the KLLs, which energetically favors a state with one conduction electron per lattice site, we find that the occupation number of the

KLLs is closer to one than the occupation of the NILs. However, as the spatial symmetry along the superlattice structure is broken from the beginning by constructing the superlattice, there occurs no phase transition, but the charge density wave corresponds to the superlattice structure.

V. CONCLUSION

We have calculated properties of f -electron superlattices. We have elucidated the question, what happens to the full gap of the isolated Kondo lattice layer, when it is inserted into a metallic host. We have shown that due to tunneling of electrons from the metallic layer into the Kondo lattice, the full gap of the isolated KLL is changed into a pseudo gap. However, by coupling the KLLs to the NILs, not only the DOS of the KLL is changed. We have demonstrated that the Kondo effect of the f -electrons also has strong influence on the non-interacting layers, which show pronounced peaks or dips at the Fermi energy. Remarkably, these peaks and dips in the NILs are strongly influenced by interference between the f -electron layers. While the configurations with an odd number of NILs show a constructive interference, which enhances the resonance at the Fermi energy, an even number of NILs results in a destructive interference, canceling all visible effects of the Kondo effect on the DOS at the Fermi energy in the (1,2)-superlattice. The Kondo effect also strongly affects the conductivity at low temperatures. Because of the formation of the Kondo gap in the KLLs, the superlattice becomes strongly anisotropic at low temperatures. Decreasing the temperature below the Kondo temperature, the out-of-plane conductivity vanishes, while the in-plane conductivity stays metallic.

In this study, we have shown that the Kondo effect plays an important role in the superlattice, not only in the f -electron layers, but also in the NILs. The possibility to tune the physical properties such as the behavior of the Kondo effect is one of the advantages of a superlattice. So far, we have only analyzed the paramagnetic state. If magnetically ordered states are analyzed, besides the Kondo effect the RKKY interaction will also become important. For weak coupling strengths, the RKKY interaction will be stronger than the paramagnetic Kondo screening, which will result in a magnetically ordered state. However, the heavy fermion materials which have been used in the experiments, i.e. CeIn_3 and CeCoIn_5 , show large regions in the pressure-temperature phase diagram, where the paramagnetic heavy-fermion state is stable. Our results, which we have shown here, can be expected to be valid for this paramagnetic heavy fermion phase, where the Kondo screening is stronger than the RKKY interaction. Because the Kondo effect in competition with the RKKY interaction plays an important role in f -electron materials, we expect that the tunability of the superlattice will result in intriguing phase diagrams including magnetic phases, which depend on the struc-

ture of the superlattice. Including magnetic phases into our studies is left as a future project.

We have focused here on artificially created f -electron superlattices. However, there are many naturally occurring layered f -electron materials, e.g. CeCoIn₅. The described consequences of the Kondo effect on the system, i.e. resonances in the DOS at the Fermi energy, can be expected to also play an important role in these compounds. This is currently under investigation.

Acknowledgments

RP and NK thank the Japan Society for the Promotion of Science (JSPS) for the support through its FIRST

Program. NK acknowledges support through KAKENHI (No. 22103005, No. 25400366). YT is supported through KAKENHI (No. 23840009). The numerical calculations were performed at the ISSP in Tokyo and on the SR16000 at YITP in Kyoto University.

-
- * peters@scphys.kyoto-u.ac.jp
- ¹ H. Shishido, T. Shibauchi, K. Yasu, T. Kato, H. Kontani, T. Terashima, and Y. Matsuda, *Science* **327**, 980 (2010).
 - ² Y. Mizukami, H. Shishido, T. Shibauchi, M. Shimozawa, S. Yasumoto, D. Watanabe, M. Yamashita, H. Ikeda, T. Terashima, H. Kontani, et al., *Nat. Phys.* **7**, 849 (2012).
 - ³ S. K. Goh, Y. Mizukami, H. Shishido, D. Watanabe, S. Yasumoto, M. Shimozawa, M. Yamashita, T. Terashima, Y. Yanase, T. Shibauchi, et al., *Phys. Rev. Lett.* **109**, 157006 (2012).
 - ⁴ S. Doniach, *Physica B* **91**, 231 (1977).
 - ⁵ P. Coleman, *Handbook of Magnetism and Advanced Magnetic Materials* (John Wiley and Sons, 2007), p. 95.
 - ⁶ P. Coleman and A. Schofield, *Nature* **433**, 226 (2005).
 - ⁷ P. Gegenwart and Q. Si, *Nature Physics* **4**, 186 (2008).
 - ⁸ C. Lacroix and M. Cyrot, *Phys. Rev. B* **20**, 1969 (1979).
 - ⁹ P. Fazekas and E. Muller-Hartmann, *Z. Phys. B: Condens. Matter* **85**, 285 (1991).
 - ¹⁰ K. Wilson, *Rev. Mod. Phys.* **47**, 773 (1975).
 - ¹¹ R. Bulla, T. Costi, and T. Pruschke, *Rev. Mod. Phys.* **80**, 395 (2008).
 - ¹² A. Georges, G. Kotliar, W. Krauth, and M. Rozenberg, *Rev. Mod. Phys.* **68**, 13 (1996).
 - ¹³ M. Jarrell, H. Aklhaghpour, and T. Pruschke, *Phys. Rev. Lett.* **70**, 1670 (1993).
 - ¹⁴ S.-J. Sun, M.-F. Yang, and T.-M. Hong, *Phys. Rev. B* **48**, 16127 (1993).
 - ¹⁵ M. J. Rozenberg, *Phys. Rev. B* **52**, 7369 (1995).
 - ¹⁶ P. Sun and G. Kotliar, *Phys. Rev. Lett.* **95**, 016402 (2005).
 - ¹⁷ R. Peters and T. Pruschke, *Phys. Rev. B* **76**, 245101 (2007).
 - ¹⁸ L. De Leo, M. Civelli, and G. Kotliar, *Phys. Rev. B* **77**, 075107 (2008).
 - ¹⁹ J. Otsuki, H. Kusunose, and Y. Kuramoto, *J. Phys. Soc. Jpn.* **78**, 034719 (2009).
 - ²⁰ S. Hoshino, J. Otsuki, and Y. Kuramoto, *Phys. Rev. B* **81**, 113108 (2010).
 - ²¹ O. Bodensiek, R. Zitko, R. Peters, and T. Pruschke, *J. Phys.: Condens. Matter* **23**, 094212 (2011).
 - ²² R. Peters, N. Kawakami, and T. Pruschke, *Phys. Rev. Lett.* **108**, 086402 (2012).
 - ²³ R. Peters, S. Hoshino, N. Kawakami, J. Otsuki, and Y. Kuramoto, *Phys. Rev. B* **87**, 165133 (2013).
 - ²⁴ A. Hewson, *The Kondo Problem to Heavy Fermions* (Cambridge University Press, 1997).
 - ²⁵ R. Peters, T. Pruschke, and F. Anders, *Phys. Rev. B* **74**, 245114 (2006).
 - ²⁶ A. Weichselbaum and J. von Delft, *Phys. Rev. Lett.* **99**, 076402 (2007).
 - ²⁷ T. Pruschke and R. Zitzler, *J. Phys.: Condens. Matter* **15**, 7867 (2003).
 - ²⁸ Y. Tada, R. Peters, and M. Oshikawa, in preparation.